Missing Isoscalar Monopole Strength in ^{58}Ni

D. H. Youngblood, H. L. Clark, and Y.-W. Lui
Cyclotron Institute, Texas A&M University, College Station, Texas 77843
(Received 18 August 1995)

The giant resonance region in ^{58}Ni was studied with inelastic scattering of 240 MeV α particles at small angles including 0°. It is shown that the total isoscalar monopole strength in the region $E_x = 12$ to 25 MeV is <50% of the $E0$ energy-weighted sum rule, and that the centroid of the $E0$ strength $E_{\mathrm{GMR}} > 24.8$ MeV in contrast to the $E_{\mathrm{GMR}} \approx 17$ MeV expected from systematics of other nuclei. If there is similar unobserved $E0$ strength in other nuclei, E_{GMR} for those nuclei may be significantly different from those used to extract nuclear matter incompressibility.

PACS numbers: 24.30.Cz, 25.55.Ci, 27.40.+z

The isoscalar giant monopole resonance (GMR) is of particular interest because its energy is directly related to the compressibility of nuclear matter (K_{nm}) [1]. In order to account for contributions from finite nuclei and extract K_{nm}, macroscopic analyses [2] of the GMR require that the energy of the GMR be known in nuclei over a wide range of A. However, significant monopole strength has been located [2] in only a few nuclei with $A < 90$. Only small amounts of $E0$ strength have been located in nuclei around $A = 60$. Approximately 25% of the $E0$ energy-weighted sum rule (EWSR) has been located in ^{58}Ni [3,4], and 30% in ^{64,66}Zn [5] with inelastic scattering of 130 MeV α particles. Small amounts of $E0$ strength have also been seen [3] with ^{3}He scattering, but the continuum in the ^{3}He spectra is apparently obscuring significant $E0$ strength in many nuclei [6]. However, in all of these studies, a large continuum (background?), the constituents of which were not known, was subtracted before the peak was analyzed for monopole strength. The location of the remainder of the monopole strength could not be restricted by these experiments. It might be broadly distributed over the region of the giant quadrupole resonance (GQR) and subtracted as part of the continuum, or located at excitation energies well above the GQR (or both). As the nuclear compressibility is related to the centroid of the monopole strength [$E_{\mathrm{GMR}} = (m_3/m_1)^{1/2}$, where m_k is the RPA sum rule [1,7] $m_k = \sum_n (E_n - E_0)|\langle 0|r^2|n\rangle|^2$], knowledge of the general location of this missing strength could be important for extracting K_{nm}.

All of the definitive monopole measurements have used inelastic alpha scattering with $E_\alpha \leq 130$ MeV. Unfortunately, the $(\alpha, ^5\mathrm{Li})$ and $(\alpha, ^5\mathrm{He})$ reactions with subsequent decay of the mass five products into an α particle and a nucleon produce broad peaks in the α particle spectrum which, for $E_\alpha = 130$ MeV, are in the excitation region corresponding to $22 < E_x < 46$ MeV in ^{58}Ni. These peaks would obscure GMR strength above $E_x \approx 22$ MeV.

We have studied ^{58}Ni using 240 MeV α particles where the "pickup-breakup" peaks appear above $E_x = 40$ MeV, well outside of the region where GMR strength is expected. We report here results with excellent peak-to-background ratios at small scattering angles including 0°. For the first time, it can be shown that the majority of the isoscalar monopole strength does not lie in the GR region ($E_x = 12$–25 MeV) or lower and hence must be at higher excitation energy. This results in a lower limit for E_{GMR} well above that expected from extrapolating GMR systematics from heavier nuclei or energies predicted from recent RPA calculations using interactions that reproduce GMR energies in heavier nuclei.

Beams of 240 MeV α particles from the Texas A&M K500 superconducting cyclotron bombarded a self-supporting 12.4 mg/cm^2 foil enriched to greater than 98% in ^{58}Ni mounted in the target chamber of the multipole-dipole-multipole spectrometer [8]. Beam was delivered to the spectrometer through a beam analysis system having two bends of 88° and 87° [9]. The horizontal acceptance of the spectrometer was 4°, and ray tracing was used to reconstruct the scattering angle. Data were taken with the spectrometer central angle (θ_{spec}) set at 0° and at 4°, covering the scattering angle range from 0° to 6°. The focal plane detector and calibration procedures are described in detail in Ref. [10]. ϕ is not measured, so the average angle for each bin was obtained by integrating over the height of the solid angle defining slit and the width of the angle bin. A spectrum taken near 0° (average angle 1.08°) is shown in Fig. 1. For these data, the beam (at 0°) and elastically scattered particles were stopped just in front of the detector, limiting the observed excitation energy range to $2 < E_x < 30$ MeV. Elastic and inelastic scattering data were taken for normalization with a different magnetic field setting covering $-10 < E_x < 18$ MeV. We previously reported [11] cross sections for elastic and inelastic scattering to low lying states in ^{58}Ni, and absolute cross sections were obtained from these data by normalizing to optical model calculations with potentials from Ref. [11]. The cross sections for a peak at $E_x = 4.54$ MeV in ^{58}Ni differed in the elastic and giant resonance spectra by 5% (2% net statistical error), and cross sections for the giant resonance spectra were renormalized upward 5% to account for this.

Distorted-wave Born approximation (DWBA) and optical-model calculations were carried out with the code

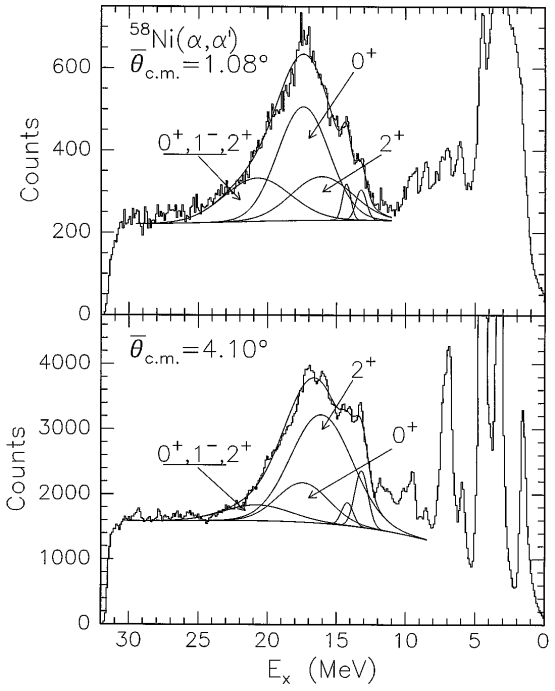

FIG. 1. Spectra obtained for ^{58}Ni(α, α') at $E_\alpha = 240$ MeV for two angles. The lines show the background and the five peak fits to the data. The dominant multipolarities in the peaks are indicated.

PTOLEMY [12] using collective form factors described by Satchler [13] and optical model parameters from Clark *et al.* [11]. Monopole and dipole form factors were calculated externally and read into PTOLEMY. The Satchler version 1 (breathing mode) form factor was used for the monopole. Input parameters for PTOLEMY were modified [14] to obtain a relativistic kinematically correct calculation. The energy-weighted sum rules are given by Satchler for the monopole and quadrupole and higher multipoles in Ref. [13], for the isovector dipole in Ref. [15], and for the isoscalar dipole by Harakeh and Dieperink [16].

The giant resonances were analyzed by subtracting a background, then doing a five peak fit [4] simultaneously to the spectra. The resulting fits are shown in Fig. 1.

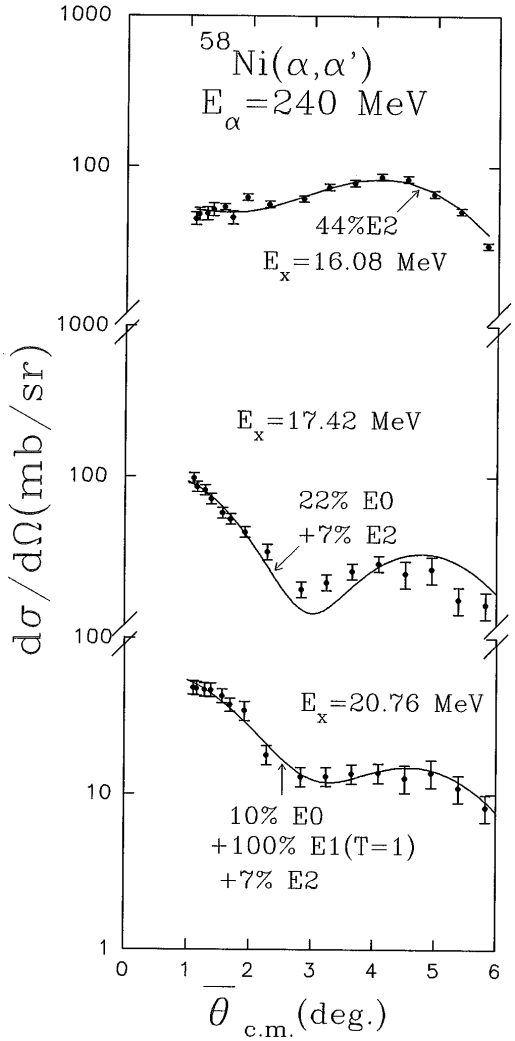

FIG. 2. Angular distributions of the differential cross sections for the broad peaks in the ^{58}Ni spectra plotted vs average center of mass angle. The lines are DWBA calculations for the multipolarities and strengths indicated.

The angular distributions obtained for the broad peaks are shown with DWBA calculations in Fig. 2. The parameters obtained, summarized in Table I, are in excellent agreement with previous measurements [2,4].

TABLE I. The % EWSR strengths extracted from DWBA fits to the cross section of the continuum for $12 \leq E_x \leq 25$ MeV, the cross section of the continuum only for $12 \leq E_x \leq 25$ MeV, and the three broad peaks only.

	% EWSR for L values					
Fit condition	0	1 ($T = 1$)[a]	1 ($T = 0$)[a]	2	3	4
Peaks and continuum $12 \leq E_x \leq 25$ MeV	28	100	30	56	20	25
Continuum only $12 \leq E_x \leq 25$ MeV	0	0	30	0	20	25
Peaks only						
$E_x = 16.08$ MeV, $\Gamma = 5.24$ MeV				44 ± 5		
$E_x = 17.42$ MeV, $\Gamma = 4.39$ MeV	22 ± 3			7^{+5}_{-3}		
$E_x = 20.76$ MeV, $\Gamma = 5.66$ MeV	10 ± 2	100		7 ± 2		

[a]Values were fixed; see text.

The angular distribution of the cross section obtained by summing the total yield from $E_x = 12$ to 25 MeV (no background subtraction) is shown in Fig. 3(a). Fits with a sum of isoscalar 0^+, 2^+, 1^-, 3^-, and 4^+, isovector 1^- resonances, and a linear (with θ) background were carried out. The result is shown by the solid line in Fig. 3(a), and parameters obtained are included in Table I. The monopole and quadrupole strengths are consistent with those found in analysis of the peaks. The isovector 1^- strength was not varied in the fits but was fixed at 100%. Strengths obtained for the isoscalar 1^-, 3^-, 4^+ components were not unique, and equally good fits could be obtained with differing combinations of these components. Variations of more than about 20% (0.2 times the strength) of the monopole component produced significantly worse fits.

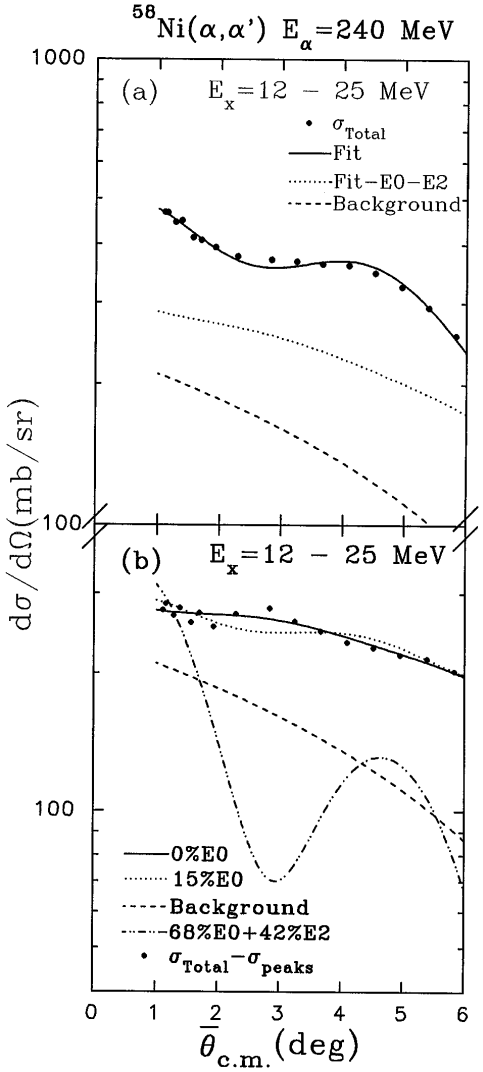

FIG. 3. (a) Angular distribution of the differential cross section for the region $E_x = 12$ to 25 MeV in ^{58}Ni plotted vs average center of mass angle. The solid line shows the DWBA calculation for the multipolarities listed in Table I. The dotted line shows the calculation with the $E0$ and $E2$ components removed. The dashed line shows the linear background assumed. (b) Angular distribution of the differential cross section for the region $E_x = 12$ to 25 MeV in ^{58}Ni, after subtraction of the contributions of the peaks, plotted vs average center of mass angle. The solid line shows the DWBA calculation for the multipolarities and strengths listed in Table I (0% $E0$ EWSR). The dotted line shows the DWBA calculation for the best fit obtained with 15% of the $E0$ EWSR included. The dashed line shows the linear background [same as in Fig. 3(a)]. The dashed–double-dotted line shows a DWBA calculation for 68% of the $E0$ EWSR and 42% of the $E2$ EWSR.

The angular distribution of the cross section for the continuum from $E_x = 12$ to 25 MeV, obtained by subtracting the cross sections of the peaks from the total cross section, is shown in Fig. 3(b). Also shown is a curve representing DWBA predictions for the $E0$ and $E2$ strength not found in the peaks (42% $E2$ EWSR + 68% $E0$ EWSR). This missing strength exceeds the continuum cross section at the smallest angles. In order to estimate the likely $E0$ strength in the continuum, several assumptions were made. We used the ansatz of a background linear in angle to model all processes other than multipole excitation in the target nucleus. This may not be a bad assumption for statistical processes, however, quasielastic scattering (knockout) should also contribute and would likely be strongly forward peaked. Thus ignoring knockout in the fits may result in an overestimate of the $E0$ strength present. First, fits including isoscalar 0^+, 2^+, 3^-, and 4^+ strength, in addition to a linear background, were made with no constraints other than limiting the strength for each component to between 0 and 100% of the EWSR. The best fit was with 0% 0^+, while χ^2 doubled if 10% of the $E0$ EWSR were included and quadrupled if 15% of $E0$ EWSR were included. $E2$ strength between 0 and 10% of the $E2$ EWSR was also indicated. Differing 3^- and 4^+ strengths were offset by different linear background parameters. The large sensitivity to 0^+ strength is due to the strongly forward peaked nature of the 0^+ angular distribution, which is not present in the data.

Multipoles higher than 4 result in essentially flat angular distributions over this angle range and could not mask the monopole. However, the angular distribution for an isoscalar dipole has a peak near the first minimum in the 0^+ and could partly mask monopole strength. The centroid energy of the isoscalar 1^- mode should be about 1.5 times the GMR energy [17], or roughly $E_x = 30$ MeV for mass 60, however, RPA calculations [18] suggest the strength will be widespread in lighter nuclei. For ^{40}Ca about 16% of the isoscalar 1^- EWSR is predicted below $E_x = 25$ MeV, while for ^{90}Zr about 46% is predicted below $E_x = 25$ MeV. For this analysis 30% of the isoscalar 1^- EWSR was assumed to lie below $E_x = 25$ MeV in ^{58}Ni. Then a good fit could be obtained if 5% of the $E0$ EWSR is present in this region (in addition to that found in the peaks), however, χ^2 doubled if 15% of the $E0$ EWSR was assumed to be in this region. If we use a doubling of χ^2 as a reasonable limit, then the region $E_x = 12$ to 25 MeV contains less than 15%

of the $E0$ EWSR in addition to that already seen in the peaks. Thus less than 50% of the $E0$ EWSR is below $E_x = 25$ MeV in ^{58}Ni. DWBA calculations for best fits assuming 0% $E0$ and 15% $E0$ are also shown in Fig. 3(b).

It is possible that the GMR in ^{58}Ni is not described well by a breathing mode form factor, and hence that DWBA calculations are giving too large a cross section. If the GMR in ^{58}Ni (and maybe other nuclei with $A < 90$) is structurally different than in heavier nuclei, possibly all of the GMR strength has been located in lighter nuclei. The only detailed guidance is from Chomaz *et al.* [19] who compared DWBA calculations for 152 MeV inelastic α scattering using microscopic form factors generated from Hartree-Fock RPA calculations with results obtained using collective form factors, and concluded that in ^{60}Ni the use of a collective form factor resulted in an underprediction of the cross section by (10–30)% for the monopole in inelastic α scattering.

If the 15% of $E0$ EWSR which might be present in the continuum is distributed uniformly between $E_x = 12$ and 25 MeV and the remaining 50% of the $E0$ EWSR is centered at $E_x = 30$ MeV with a 5 MeV width, then $E_{\mathrm{GMR}} > 24.8$ MeV in ^{58}Ni. Figure 4 shows a plot of $E_{\mathrm{GMR}}A^{1/3}$ vs A for all spherical nuclei where 100% of the $E0$ EWSR has been observed [2]. The centroid of the *observed* strength in ^{58}Ni corresponds to $EA^{1/3} = 72.1$ MeV, in reasonable agreement with the trend of other nuclei. However, this represents only 32% of the $E0$ EWSR. The lower limit for $E_{\mathrm{GMR}} = 24.8$ MeV gives $E_{\mathrm{GMR}}A^{1/3} = 96$ MeV, which is much higher than for any of the other nuclei.

The disagreement of E_{GMR} for ^{58}Ni with systematics of other nuclei may be due to the existence of an as yet unidentified $E0$ strength at higher excitation in these other nuclei. For example, the $E0$ strength in ^{90}Zr was found [2] to be (90 ± 20)% of the $E0$ EWSR. Thus as much as 30% of the $E0$ EWSR strength could be located at higher excitation. The experimental errors are similar for all of the nuclei shown in Fig. 4. In a recent microscopic approach to determine nuclear matter incompressibility from GMR energies, Blaizot *et al.* [20] explore corrections to GMR energies obtained with Hartree-Fock RPA calculations, and their results are also shown in Fig. 4. The mass dependence they obtain is somewhat different from the data. In particular, $E_{\mathrm{GMR}}A^{1/3}$ is slightly higher for ^{90}Zr than ^{118}Sn, whereas the experimental values around mass 90 are lower than at mass 118. If there is unobserved $E0$ strength at higher energies in these heavier nuclei that raises E_{GMR} significantly, then an interaction which reproduces E_{GMR} will show a correspondingly higher compressibility. If $E_{\mathrm{GMR}}A^{1/3}$ for ^{208}Pb were as high as the lower limit we obtain for ^{58}Ni (96 MeV), a simple estimate shows that the compressibility required to explain the data would be 305 MeV, rather than the 215 MeV obtained by Blaizot *et al.*

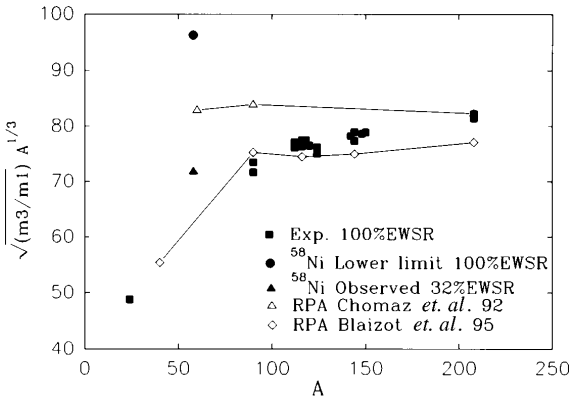

FIG. 4. $E_{\mathrm{GMR}}A^{1/3}$ is plotted vs A for nuclei where 100% of the $E0$ EWSR has been identified (squares). The solid triangle is the value obtained for ^{58}Ni using only the strength observed in this work (32% $E0$ EWSR). The solid circle is the lower limit for $E_{\mathrm{GMR}}A^{1/3}$ in ^{58}Ni for 100% of the $E0$ EWSR. Hartree-Fock RPA calculations are shown by the open triangles (Ref. [19]) and diamonds (Ref. [20]).

This work was supported in part by the U.S. Department of Energy under Grant No. DE-FG03-93ER40773 and by the Robert A. Welch Foundation.

[1] J. P. Blaizot, Phys. Rep. **64**, 171 (1980).
[2] S. Shlomo and D. H. Youngblood, Phys. Rev. C **47**, 529 (1993).
[3] M. Buenerd *et al.*, Phys. Rev. Lett. **45**, 1667 (1980).
[4] D. H. Youngblood and Y.-W. Lui, Phys. Rev. C **44**, 1878 (1991).
[5] D. H. Youngblood *et al.*, Phys. Rev. C **23**, 197 (1981).
[6] G. Duhamel *et al.*, Phys. Rev. C **38**, 2509 (1988).
[7] J. Treiner *et al.*, Nucl. Phys. **A371**, 253 (1981).
[8] D. M. Pringle *et al.*, Nucl. Instrum. Methods Phys. Res., Sect. A **245**, 230 (1986).
[9] D. H. Youngblood and J. D. Bronson, Nucl. Instrum. Methods Phys. Res., Sect. A **361**, 37 (1995).
[10] D. H. Youngblood *et al.*, Nucl. Instrum. Methods Phys. Res., Sect. A **361**, 539 (1995).
[11] H. L. Clark *et al.*, Nucl. Phys. **A589**, 416 (1995).
[12] M. Rhoades-Brown *et al.*, Phys. Rev. C **21**, 2417 (1980); M. H. Macfarlane and S. C. Pieper, Argonne National Laboratory Report No. ANL-76-11, Rev. 1, 1978 (unpublished).
[13] G. R. Satchler, Part. Nucl. **5**, 195 (1973); Nucl. Phys. **A195**, 1 (1972).
[14] G. R. Satchler, Nucl. Phys. **A540**, 533 (1992).
[15] G. R. Satchler, Nucl. Phys. **A47**, 215 (1987).
[16] M. N. Harakeh and A. E. L. Dieperink, Phys. Rev. C **23**, 2329 (1981).
[17] S. Stringari, Phys. Lett. **108B**, 232 (1982).
[18] Nguyen Van Giai and H. Sagawa, Nucl. Phys. **A371**, 1 (1981).
[19] Ph. Chomaz *et al.*, Phys. Lett. B **281**, 6 (1992).
[20] J. P. Blaizot *et al.*, Nucl. Phys. **A591**, 435 (1995).